EXPERIMENTAL INVESTIGATION OF FLAME AND PRESSURE DYNAMICS AFTER SPONTANEUS IGNITION IN TUBE GEOMETRY

Grune, J.[1*], Sempert, K.[1], Kuznetsov, M.[2], Jordan, T.[2]

[1*]Pro-Science GmbH, Ettlingen, Parkstr.9, 76275, Germany, grune@pro-science.de
[1]Pro-Science GmbH, Germany,
[2]Karlsruhe Institute of Technology, IKET, Germany

ABSTRACT

Spontaneous ignition processes due to high-pressure hydrogen releases into air are known phenomena. The sudden expansion of pressurized hydrogen into a pipe, filled with ambient air, can lead to a spontaneous ignition with a jet fire. This paper presents results of an experimental investigation of the visible flame propagation and pressure measurements in 4 mm extension tubes of up to 1 m length attached to a bulk vessel by a rupture disc. Transparent glass tubes for visual observation and shock wave pressure sensors are used in this study. The effect of the extension tube length on the development of a stable jet fire after a spontaneous ignition is discussed.

1. Introduction

Hydrogen is used in industry in many different applications. Accidental hydrogen releases from pipe systems are one of the main hazards that occur in the handling of pressurised hydrogen. It was shown, in [1] [2] [3] [4] and other publications, that in case of a sudden hydrogen release from a high pressure initial state into air self-ignition may occur if downstream the rupture location an extension pipe is present. For safety applications and assessment this is important if the ignition inside the tube leads to a fully developed jet fire in the ambient with the possibility to generate pressure and thermal loads [5]. In experimental observations three cases are distinguished, no ignition (no ignition), ignition with quenching of the reaction on the nozzle exit (failed ignition) and the self-ignition of the released hydrogen with a fully developed jet fire (ignition).
All experimental set ups which were used for the studies of the phenomena on spontaneous ignition due to sudden release of pressurised hydrogen in air can be described as an open-end shock tube performance with pressurised hydrogen as driver and ambient air as driven gas. Due to the ruptured membrane the compressed hydrogen suddenly comes in contact with the ambient air. The rapidly expanding hydrogen compresses the air and produces a shock wave. The leading shock wave propagates inside the tube and heats up the region behind the shock and may ignite the mixture which is formed on the contact surface between the two gases. The ideal shock tube theory is not able to explain the experimentally observed ignition events at the sudden release through a thin pipe [5]. The theoretical temperature increase is too low to ignite the mixture in the residential time of the mixing zone inside the tube. It is assumed that inside miniature shock tubes other phenomena like boundary layer effects or reflection of shock waves are responsible for high temperature regions behind the shock. Brouillette [6] used a miniature shock tube (d = 5.3 mm) and low air pressure in the driven sector to simulate the effect of small scale. Duff [7] studied the shock tube performance at low initial pressures and summarised that the shock-tube performance at low initial pressure is more nearly approximated by a complicated pipe flow than by a one dimensional shock-tube theory. In both studies helium as fastest driven gas was used. With hydrogen as driver gas and atmospheric air as driven gas in miniature scale tubes non-ideal shock-tube behaviour is

expected. Pressure measurements combined with light sensor signals from miniature shock-tube tests were presented in [3] [4] [8] and in combination with optical high speed technique in [9]. However there is a lack of highly resolved pressure measurements in miniature shock tubes with spontaneous ignition due to the sudden discharge of pressurised hydrogen into air. The goal of this work is to measure the pressure dynamic in 4 mm circular extension tubes downstream a rupture disc in combination with a visualisation of the radiating (reacting) zone in case of a spontaneous ignition due to the sudden release of pressurized hydrogen into atmospheric air.

2. Experimental set-up

The miniature open end shock tube facility is sketched in Fig. 1 top left. Via a feed line valve (a) the cylindrical storage vessel (b) with a volume of 0.37 dm^3 is filled with pressurized high purity H_2 (99.999 vol. %). A helium driven needle valve DN 4 mm (c) with a valve opening time < 2 ms is installed between the high pressure vessel and a 4 mm release nozzle (d). The release nozzle is equipped with a rupture disc holder build from 4 mm tubes, see inserted picture. The extension pipe downstream of the rupture disc is open to the atmosphere. In the presented study different 4 mm cylindrical extension tubes are used in the experiments. The Fig. 1 (bottom) shows an exemplary extension tube configuration. The total extension tube length in this example is 630 mm, three pressure sensor ports (e) are connected via industrial fittings with glass tubes (f). The pressure sensor ports are equipped with dynamic tourmaline gauges (PCB Type 134A24). The active planar sensor surface is integrated in the 4 mm pipe on the inner tangential position in the best way to avoid disturbances of the shock wave or the high speed flow. The sensor signals are monitored with a sample rate of 1 µs. This value is five times higher than the sensors rise time of 0.2 µs. Aluminum rupture discs from 0.06 mm up to 0.3 mm were used in the experiments. Fig 1 right shows the burst pressure range of the used aluminum membranes and the initial release pressures P_0 in the vessel used in this study.

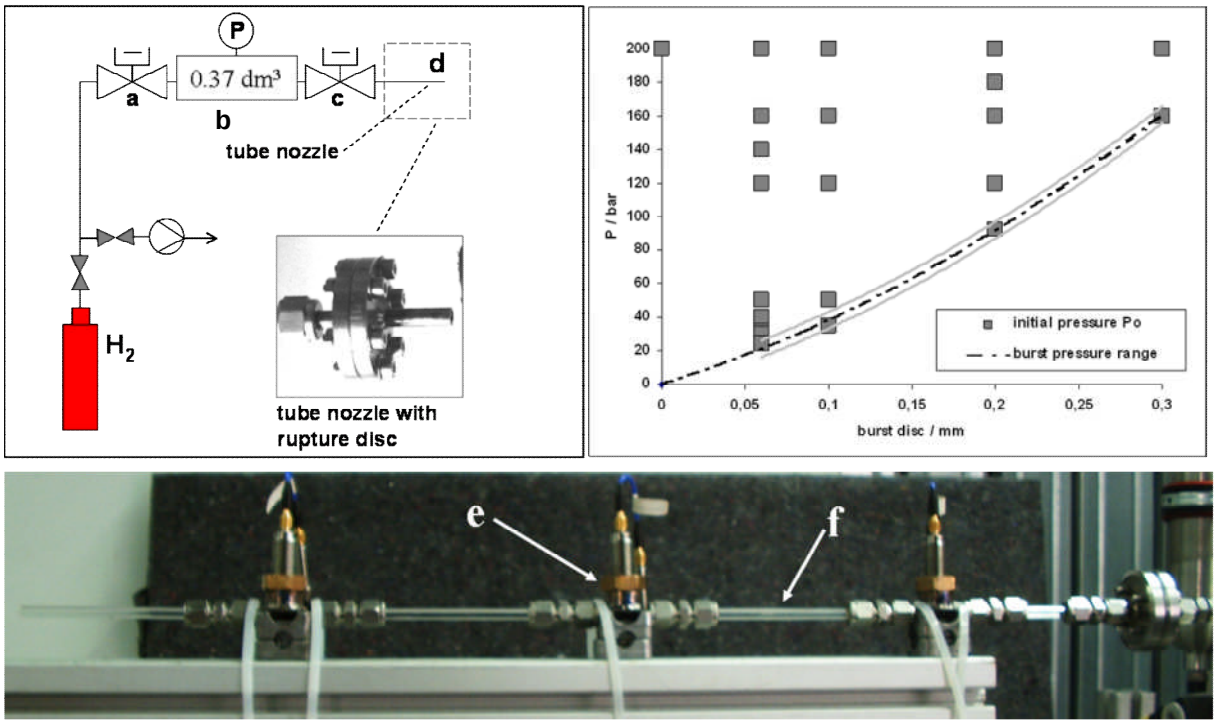

Fig.1: Schematic of the experimental set-up (top left). Burst pressure range of the aluminum membranes vs. initial bulk pressure (top right). Photograph of a 4 mm extension tube built from three pressure gauges in metal tubes and transparent glass sections (bottom).

In most cases the rupture pressure of the installed aluminum rupture discs was significantly lower than the bulk pressures P_0 in the 0.37 dm^3 vessel. In all experiments the small volume of 2.2 cm^3 between the rupture disc and the fast bulk release valve (c) was filled with H_2 at atmospheric pressure.

In Table 1 the main experimental variables: extension tube configuration, release pressure in the 0.37 dm^3 vessel and the rupture disc properties are listed. Ignition events and flame propagation inside the extension tube were captured via high speed cinematography along the transparent tube parts. A resulting fully developed jet fire was observed by direct optical observation.

Table 1: Overview of the main experimental variables.

Range of bulk pressure P_0 / bar	**Range of rupture disc thickness s / mm**	**Total tube lengths L_{total} / mm**	**Position pressure gauge P1 L_{P1} / mm**	**Position pressure gauge P2 L_{P2} / mm**	**Position pressure gauge P3 L_{P3} / mm**	**Transparent tube parts**
0 to 200	0.0 to 0.3	132	80	122	-	-
50 and 200	0.0 and 0.1	1145	1093	1135	-	yes
25 to 200	0.06 to 0.3	645	593	635	-	yes
200	0.0 to 0.3	230	68	133	202	-
30 to 200	0.0 to 0.2	630	133	309	490	yes
50 and 120	0.06 to 0.2	720	52	581	-	yes
120 to 240	0.1	1040	52	-	-	yes
24 to 160	0.06 to 0.3	210	122	70		yes
120	0.06	633	52	133	494	yes

3. Experimental observations

3.1 Flow visualisation in rectangular tubes

The shadow pictures taken from a high speed movie (100000 f/s) in Fig. 2 illustrate qualitatively the release of pressurised hydrogen (60 bar) into a rectangular 5 mm tube filled with ambient air via rupture of an aluminium membrane (0.1 mm). In this example the visible zone starts from the position of the burst membrane (A). The burst membrane ruptures within the first 10 µs and at first a relatively slow wave with the velocity of the sound speed in air propagates inside the tube. But later in time, 40 to 50 µs after the membrane was completely ruptured, it is not possible to separate a leading shock from the expanding hydrogen. After 60 µs a leading shock front (C) followed by a contact surface (D) can be identified. The distance between the leading shock front (C) and contact surface (D) increases with the distance. The leading shock front is not captured as a sharp line in this shadow graph because the structure of the shock wave is not ideal planar it is in a three-dimensional form. Between the leading shock front and the contact face multiple reflecting shock waves are visible. Due to the high speed flow (~ 1000 m/s) in the relatively narrow tube boundary layers (F) are visible near the tube walls. Some particles (E) from the destroyed aluminium membrane travel with the flow later in time. Similar flow visualisation pictures captured in 10 mm rectangular tubes are presented in [9] were the first 37 mm downstream the membranes were blocked by the window frame. The region in a short distance downstream the membrane, where the main shock wave is formed by the complex start-up of the hydrogen expansion synchronic with ruptured membrane, was investigated experimentally via pressure measurements in a 18 mm tube in [8]. It can be assumed that the three-dimensional rupture of the membrane and the complex formation of the high speed H_2-flow are responsible for a fast gas mixing in the start

up. Further it is observed that a minimum distance of 2 to 3 tube diameters is necessary for the formation of a relatively planar leading shock.

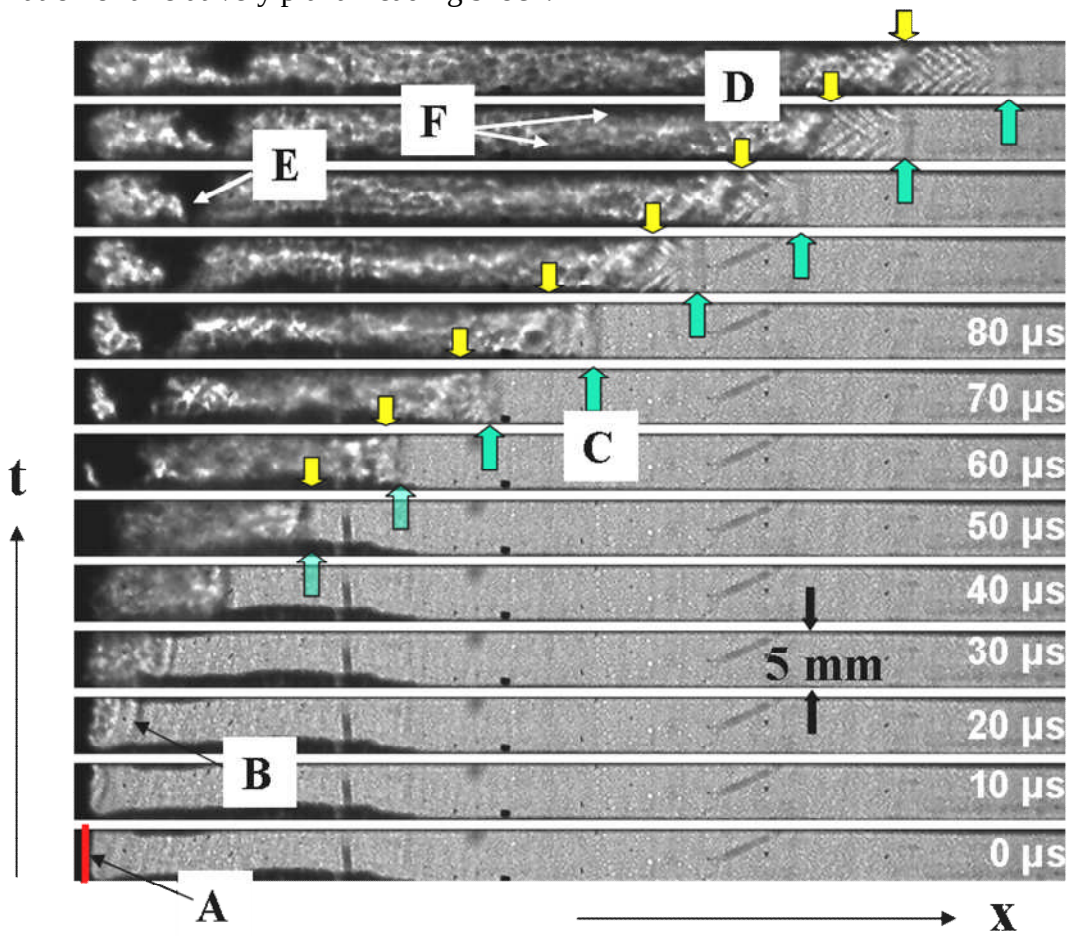

Fig. 2: Flow visualisation via shadow graphs in a rectangular 5 mm tube.

The process directly after the start up of the membrane rupture plays a key role for the possibility of an ignition event due to the sudden hydrogen release into an oxidizing atmosphere. Experimental investigations of very fast and three dimensional complex processes in miniature scale are very difficult and there are also differences between rectangular and circular tubes. Optical observations from rectangular tubes can not be transferred to circular tubes. In the following study a 4 mm circular rupture disc holder was used in all experiments. This device was also used in [5] and it is approved to ignite successfully and reproducible. It can be assumed that the design of the extension tube, a connection of several tube segments via industrial fittings, promotes and supports the ignition events.

3.2. Pressure dynamic in 4 mm circular tubes

The initial flow released via the opening of the leak valve (Fig. 1) into the release nozzle accumulates first gas upstream the rupture membrane which blocks the nozzle pipe up to the point of the membrane rupture. Fig. 3 shows the pressure histories of a gauge located 68 mm downstream the rupture disc for an initial bulk pressure of 200 bar and different membrane thicknesses. Without membrane the pressure increase is relatively constant with time. A ruptured membrane in the flow path produces a fast increasing pressure profile inside the extension tube. The amplitudes and the arrival times increase with the thickness of the

membrane. But later in time the maximum pressure level (~ 60 bar) becomes equal for all examples.

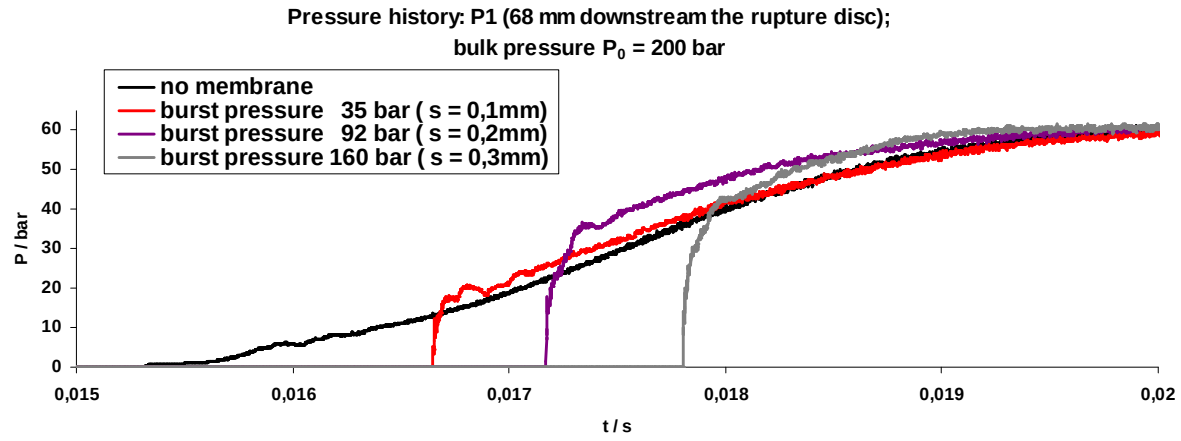

Fig. 3: Pressure histories in a position 68 mm downstream the rupture disc for 200 bar initial bulk pressure.

In Fig. 3 the original time scale is used which includes the pre-activation time of the fast valve. Fig. 4 shows pressure histories of a gauge located 133 mm downstream the rupture disc for an initial release pressure of 120 bar and membranes with a burst pressure of ~ 35 bar.

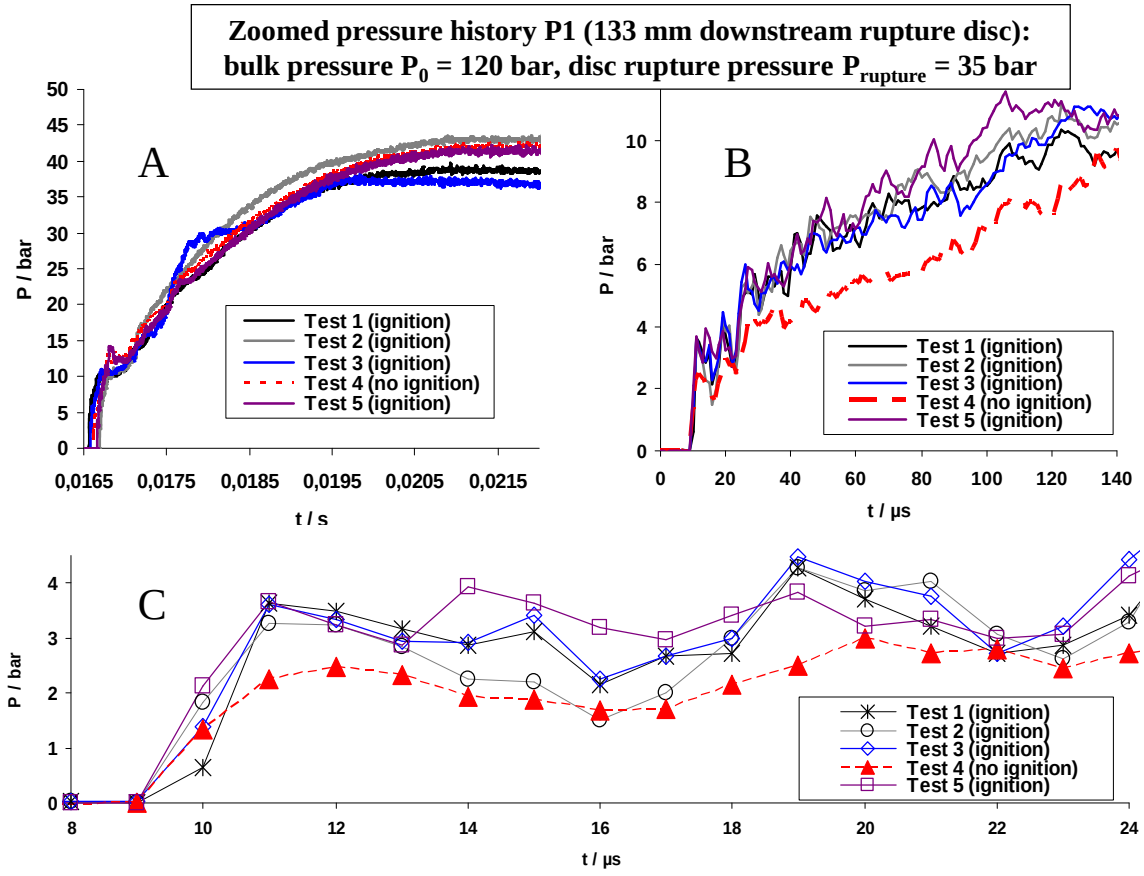

Fig. 4: Pressure histories in a position 133 mm downstream the rupture disc for 120 bar initial release pressure.

The experiments were performed five times with the same initial conditions. The plot Fig. 4 (A) shows the pressure histories of the five tests (no. 1 to no. 5) in a coarse rough time scale up to the maximum pressure. At first the pressure rise is relative sharp to a level of ~ 10 bar and later in time continually to the maximum of ~ 40 bar. All five pressure histories look very similar. Only in the test no. 4 no ignition event was observed. In Fig. 4 (B) the regions of the first sharp pressure rise are zoomed out, the first pressure jump of the sensor is set to t = 10 µs for all experiments. This graph resolves a relative weak shock wave with amplitudes of less than 4 bar and a constant increase of the pressure to a level of 10 bar within a time of ~ 100 µs. In this plot the pressure level of the test no. 4, which leads not to an ignition event, lies clearly below the four others. In the Fig. 4 (C) the leading shock wave is zoomed out to microsecond range for the five tests. As rise time of the shock wave a value of less than 2 µs is visible for all tests and the reached pressure level is more or less constant for more than 14 µs. The pressure level measured in test 4 lies below the values measured in the other tests, so it can be assumed that a bad membrane is responsible for the non-ignition event in test 4. The measured shock wave velocities in these experiments lie between 814 m/s (test 4) and 920 m/s (test 5) so that a flight time of 14 µs corresponds to roughly 12 mm in distance, which is three times the tube diameter.

Fig. 5 shows the pressure histories for an experiment with an initial bulk pressure of 200 bar and a membrane rupture pressure of 90 bar for three different locations along the 630 mm long extension tube. The pressure history P1, measured in a distance of 129 mm downstream the membrane, shows qualitatively the same behaviour as the curves in Fig. 4 B. After a shock wave a pressure plateau for a short time is reached before the pressure increases again. The pressure history P2 in a distance of 349 mm downstream the membrane shows a 1onger duration time of the pressure plateau, which was reached after the first shock, and afterwards the increase of the pressure is almost linear with time. The pressure signal recorded in a distance of 590 mm downstream the membrane shows a distinct pressure plateau with a duration of more than 80 µs after the first shock. The shock wave velocities measured in this experiment lie at 1630 m/s between gauge P1 and P2 and at 1560 m/s between gauge P2 and P3 and the experiment lead to a jet fire. With increasing distance from the source of the shock wave the amplitude of the shock wave decreases as well, remarkable is that the second maximum in Fig. 5 reaches the same level independent of the location of the sensor.

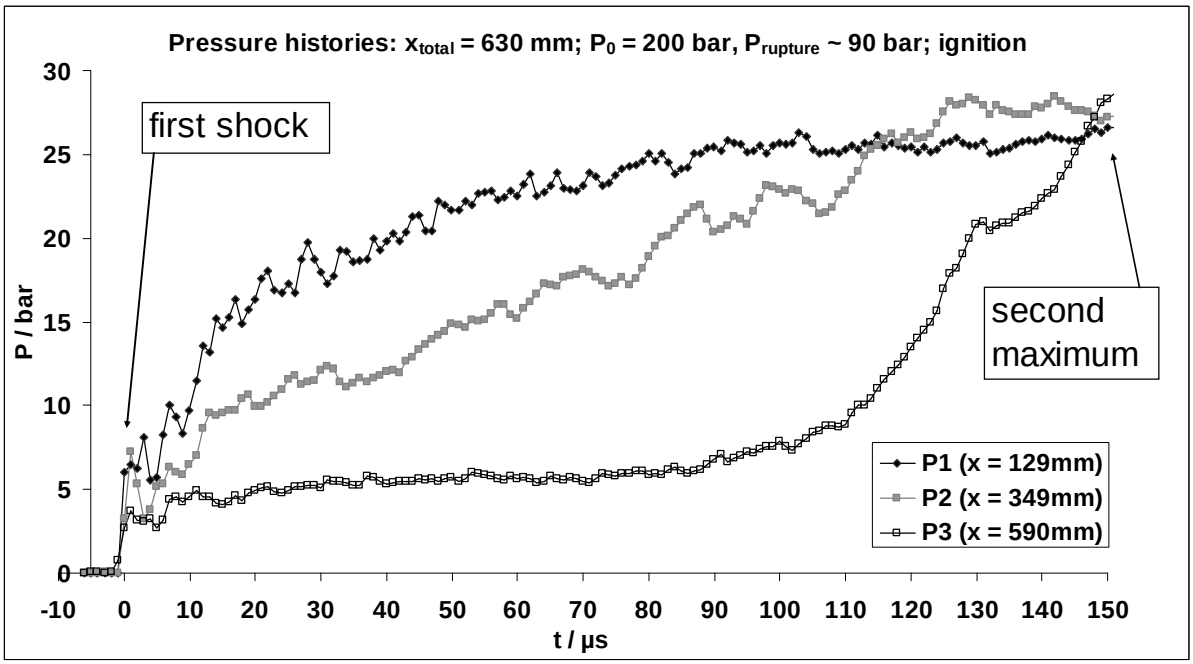

Fig. 5: Pressure histories for 200 bar initial bulk pressure in different positions downstream the rupture disc.

In all pressure histories measured in this study two prominent points were identified, the level of the leading shock wave (first shock) and the level of the second compression afterwards (second maximum), as marked in Fig 5. These two characteristic pressure levels are plotted in Fig. 6 left over the shock wave velocity for all experiments in this study. The shock wave velocities correspond to the flight time of the shock wave between two gauges. The measured first shock wave value increases only slowly with the increase of its velocity. The second maxima increase faster with the increase of the velocity. On the right side of Fig. 6 the ratio between the second maximum and the first shock is plotted over the shock wave velocities. It can be seen that with increasing shock wave velocity in the range from 400 m/s to 1000 m/s the ratio of the prominent pressure levels decreases linearly from 12 to less than 4. For shock wave velocities above 1000 m/s the ratio is constant. This break of the slope separates the experiments with ignition events from experiments without ignition only in one direction. Ignition events and no ignition events were observed in case of shock wave velocities below 1000 m/s, but for shock wave velocities above 1000 m/s only ignition events are present.

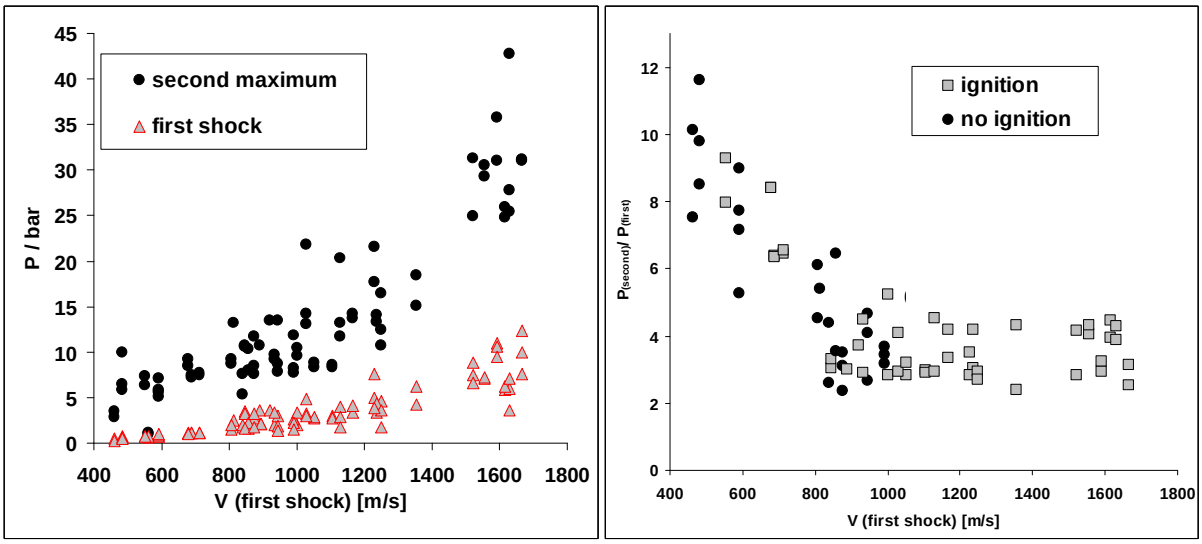

Fig.6: Left, summary of the two characteristic pressure levels (first shock and second maximum) and shock wave velocity. Right, ratio of the two characteristic pressure levels versus shock wave velocity.

The reason for the relative wide scattering of the data points in Fig. 6 is the wide range of tube lengths and the different sensor positions which were used in this study. A plot of the initial bulk pressure P_0 or the rupture pressure $P_{(rupture)}$ of the membrane and the two derived prominent points from the measured pressure histories leads to wide scattering point diagrams. A relative simple and reasonable correlation between the initial bulk pressure P_0 and the rupture pressure $P_{(rupture)}$ of the membrane was found analytically by the use of the product of its roots. Fig. 7 shows the correlations of the amplitudes of the first shock and the second pressure maximum to the product of the square roots of the initial release pressure P_0 and the rupture pressure $P_{(rupture)}$ of the membrane.

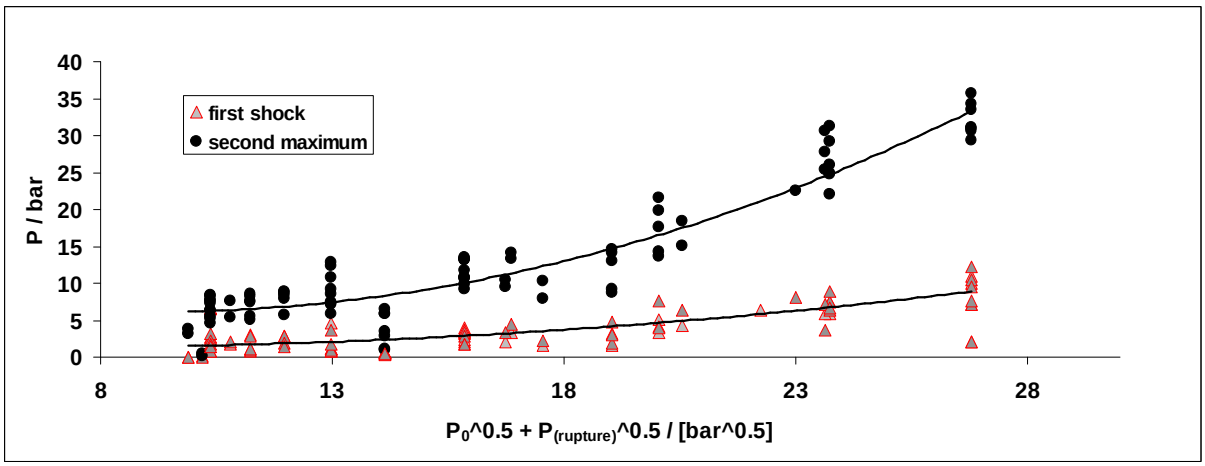

Fig. 7: Correlation of the amplitudes of the first shock and the second pressure maximum to the initial bulk pressure P_0 and the rupture pressure $P_{(rupture)}$ of the membrane.

3.3. Flame propagation after spontaneous ignition in 4 mm circular tubes

Due to the design of the membrane holder the transparent range downstream the rupture disc starts in a distance of minimum 52 mm in all configurations. In the experiments in which glass tubes were installed all observed ignition events took place in the first 52 mm downstream the membrane. The picture series in Fig. 8 shows the visible flame propagation in the extension tube (configuration as presented in Fig. 1). The bulk pressure P_0 was 50 bar and the burst pressure of the 0.1 mm membrane was ~35 bar.

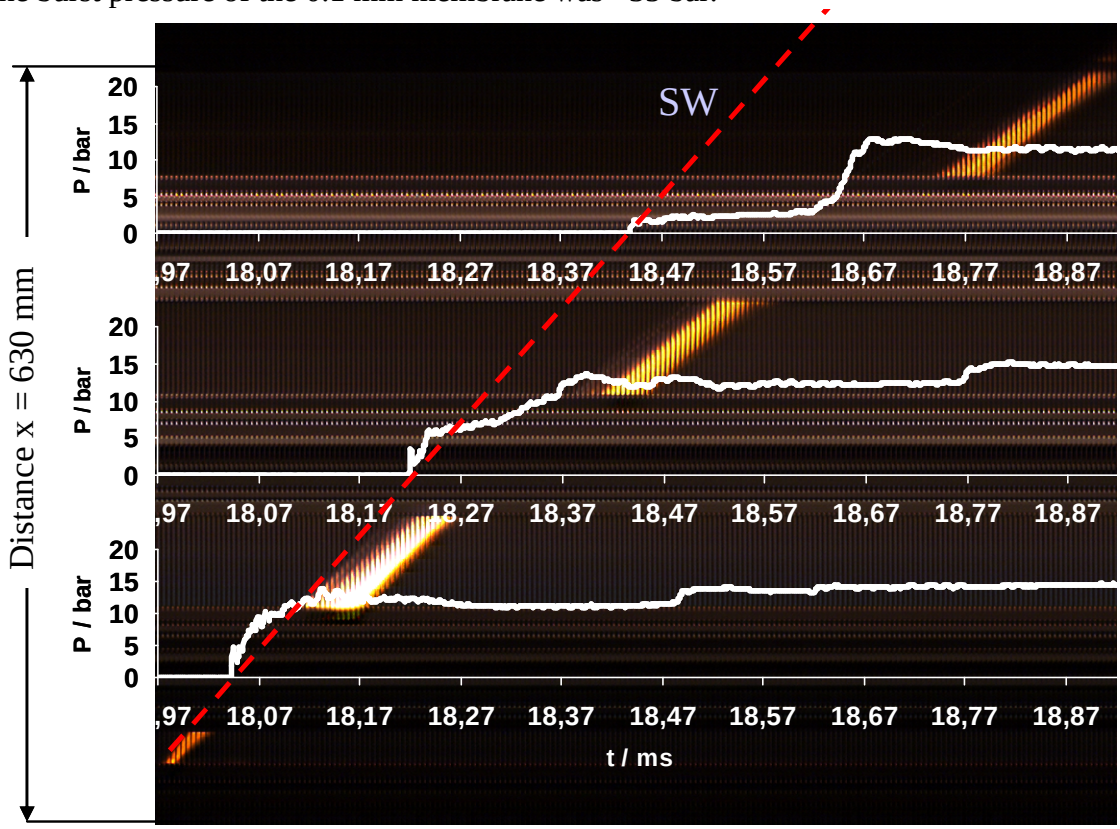

Fig. 8: Flame propagation and pressure history (P_0 = 50 bar; $P_{(rupture)}$ = 35 bar).

The pressure records were placed and scaled according to their positions along the tube. The ignition takes place in the invisible first 52 mm downstream the membrane. The leading shock (SW) shows linear dependencies in this time-distance diagram. The luminescence of the reaction shows a decaying velocity with increasing time and distance. The center of the luminescence lies in the region of the position of the second pressure maximum. Due to the optical properties of the circular 4 mm glass tubes the visible luminescence inside the tube broadens for an outside observer forwards and backwards of its original position. This effect produces the optical displacement due to the immersion of the luminescence into the metal parts and on its exhaust.
In the flame propagation path shown in Fig. 9 the visible section is not blocked by gauge holders. The bulk pressure P_0 was 200 bar and the burst pressure of the 0.3 mm membrane was 160 bar. The ignition takes place in the invisible first 52 mm downstream the membrane. The visible flame fans out with increasing time and distance up to a point when the flame branches into two directions. The first direction is coupled to the leading shock, the second direction follows the position of the second pressure maximum which presents the main contact surface. The leading visible flame zone, which propagates closely behind the leading shock quenched soon after the branch point of the flame was reached. The flame that propagates with the contact surface burns longer and reaches the exhaust of the pipe in all cases. The intensity of the luminescence decreases with the flight time and does not lead to a jet fire on the nozzle exit.

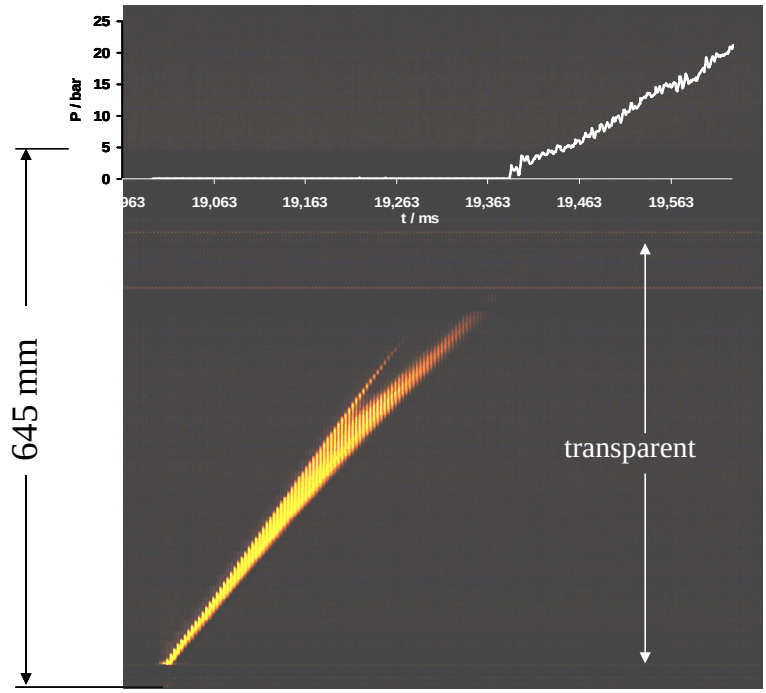

Fig. 9: Flame propagation and pressure history (P_0 = 200 bar; $P_{(rupture)}$ = 160 bar).

In the time-distance diagram of Fig. 10 the flame propagation and a synchronized pressure history are shown for an experiment in a 720 mm long tube. The flame branch point, the leading shock and the second pressure maximum is visible. Additionally the propagating particles from the ruptured membrane illustrate the high speed flow inside the tube.
In all cases where the extension tube was longer than the distance to the flame branch point no jet fire on the nozzle exit was as observed. Only the closed fan out of the reaction zone is able to ignite the released hydrogen on the nozzle exit.

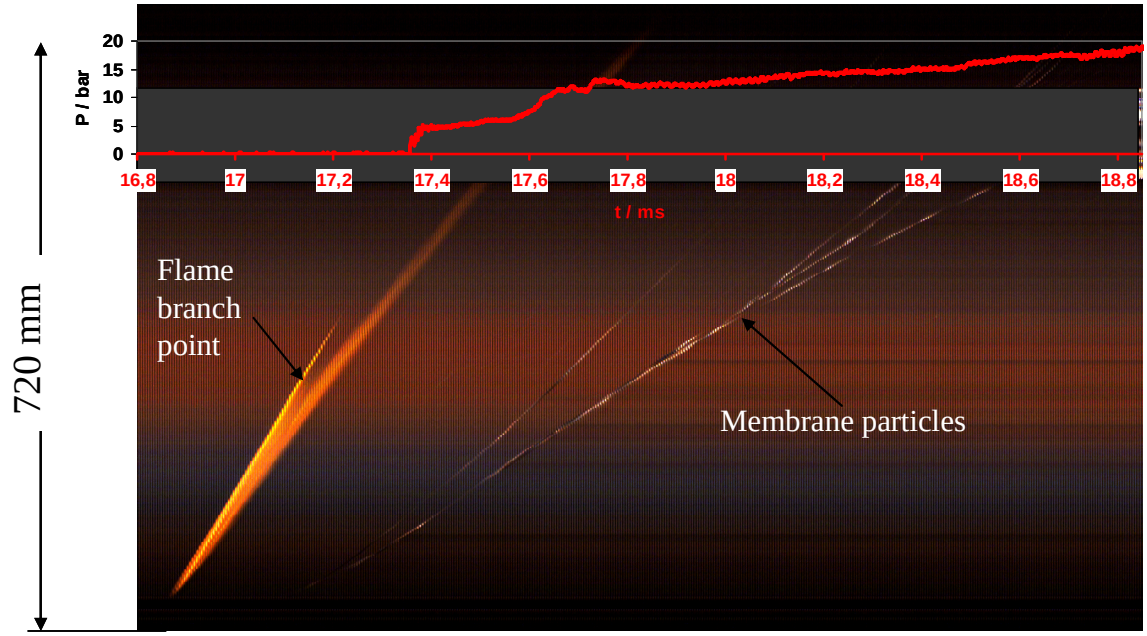

Fig. 10: Flame propagation and pressure history (P_0 = 120 bar; $P_{(rupture)}$ = 35 bar).

4. Discussion

The results of the pressure measurements inside the 4 mm extension tubes downstream the rupture disc show non ideal shock tube behaviour. The measured pressure histories show a certain similarity with the densitometer traces presented in [7] and the pressure histories in [6] where the driver gas flow has an influence on the shock wave amplitude value. Also the pressure histories captured in a 5 mm cylindrical tube presented in [3] indicate a non ideal shock tube behaviour. The circumstances that in the present study the H_2 release pressure (bulk pressure) was mostly higher than the rupture resistance of the membranes supports together with the relatively large driver gas volume the competition of the high speed flow (contact surface) and the leading shock front. Especially in the start up phase of the membrane rupture where the source of an effective gas mixing and the formation of a hot spot is expected. For a successful self-ignition event during the sudden hydrogen release from a high pressure initial state into air the presence of a hot spot with a sufficient high temperature in an ignitable mixture cloud is necessary. When a hot spot is present, it propagates fast with the high speed flow to the exhaust, the ignition time is limited to the residential time of the hot spot inside the extension tube downstream the rupture disc.
Based on the results of the dynamic pressure measurements, with a leading shock wave followed by a second compression, the temperature increase in the mixing zone can be formulated as a two step procedure. At first the leading shock wave heats up the gas temperature from T_U to T_{sw} (Eq. 1 (normal shock wave)). In the second step an adiabatic compression from the pressure level $P_{\text{first shock}}$ to $P_{\text{second maximum}}$ increases the temperature from T_{SW} to the maximum temperature T_{max} (Eq. 2).

$$T_{SW} = \frac{T_U(2\cdot\gamma\cdot M^2)\cdot((\gamma-1)\cdot M^2+2))}{(\gamma+1)^2\cdot M^2} \quad \text{(Eq. 1)} \qquad T_{\max} = T_{SW}\cdot\left(\frac{P_{\text{sec}ond\,\max imum}}{P_{firstshock}}\right)^{\left(\frac{\gamma-1}{\gamma}\right)} \quad \text{(Eq. 2)}$$

Where γ is the ratio of specific heat; M is the Mach number (air); T_U is the ambient temperature; T_{sw} is the temperature reached behind the first shock; T_{max} is the maximum temperature; $P_{first\ shock}$ is the pressure level of the first shock and $P_{second\ maximum}$ is the pressure level of the second maximum.
In Fig. 11 the calculated maximum temperatures T_{max} using Eq. 1 and Eq. 2 are plotted over the residential time of the shock wave in the extension tube for the experiments in this work and previous measurement data [5]. To derive the necessary data from [5] the correlations in Fig. 6 and Fig. 7 were used. Additionally calculated values of ignition delay times vs. temperatures for H_2/air-mixtures are plotted with a time shift of 10 µs in the diagram. The initial conditions for the calculations using Cantera code [10] with Lutz mechanism [11] were 1 bar and 20 ° C.

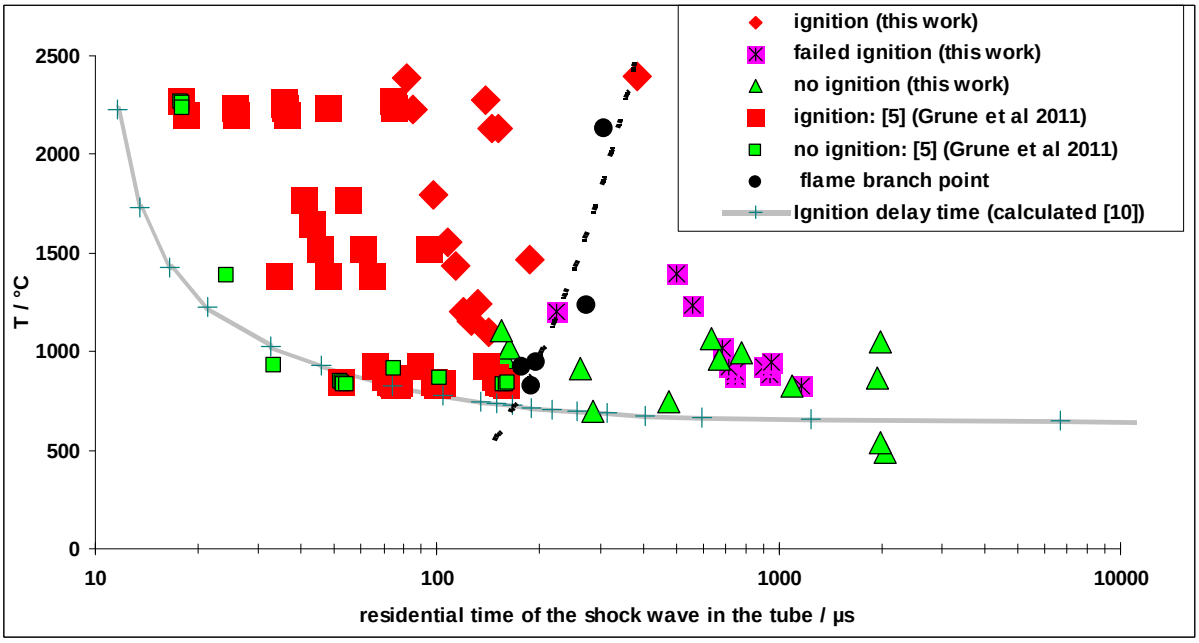

Fig. 11: Summarized mapping of the experimental results from different tube lengths, membrane thicknesses and initial bulk pressures and calculated ignition delay time.

Fig. 11 summarizes the experimental results from different tube lengths, membrane thicknesses and initial bulk pressures. All ignition events are located above the calculated and time shifted (+ 10 µs) ignition delay time. A minimum residential time of ~ 18 µs for the shock wave in the extension tube is necessary to ignite the mixture, for a wave velocity of 1500 m/s a tube length of 27 mm is necessary to form the conditions for an ignition event. For longer tubes (longer residential times of the shock wave) the possibility for a failed ignition on the nozzle exhaust is present. The time when the flame branch point inside the extension tube is reached (black points) separates the ignition events with resulting jet fire from the cases without a resulting jet fire (failed ignition).
The summarized mapping of the experimental results shows all important boundaries for the self-ignition in the studied case. Minimum lengths of the extension tube to form the important conditions (gas mixing and formation of the shock wave) for an ignition are required as well as a minimum temperature increases to ignite the mixture. Additionally a separation line of self-ignition events with jet fire (ignition) or no jet fire (failed ignition) on the nozzle exhaust is plotted.

5. Conclusions

This work presents an experimental investigation of the pressure dynamic in 4 mm circular extension tubes downstream a rupture disc in combination with the visualisation of the reacting zone in case of a spontaneous ignition due to the sudden release of pressurised hydrogen into atmospheric air.
A spontaneous ignition due to the sudden release of pressurized hydrogen into atmospheric air was observed for a H_2 release overpressure of 30 bar in combination with a membrane (rupture pressure of 24 bar) inside a 645 mm long extension tube. In a shorter extension tube (42 mm) the limit for an ignition was found to be 25 bar [5]. All ignition events observed in the present study were initiated in the first 52 mm downstream the rupture membrane. The flame fans out with increasing distance of the flow in the nozzle exhaust direction. In long tubes a branching of the flame fan out in two directions was observed, the first direction is coupled to the leading shock, the second direction follows the position of the main contact surface. If the extension tube is longer than the position where the point of the flame branching takes place no jet fire on the nozzle exit was observed.
The pressure histories measured inside the extension tubes downstream of the rupture membrane show non ideal shock tube characteristics. Two prominent points were identified, the level of the leading shock wave (first shock) and the level of the second compression afterwards (second maximum). Temperature increase by the first shock wave followed by adiabatic compression, demonstrates the possibility for a successful self-ignition event during the sudden hydrogen release from a high pressure initial state into air for the described miniature open end shock tube.

References

[1] Wolanski P, Wojcicki S. Investigation into the mechanism of the diffusion ignitron of a combustible gas flowing into an oxidizing atmosphere. In: Proc 14th Comb Symp; 1973. pp. 1217-1223.

[2] Dryer FL, Chaos M, Zhao Z, Stein JN, Alpert JY, Homer CJ. Spontaneous ignition of pressurized releases of hydrogen and natural gas into air. Comb Sci Techn 2007;179:663-694.

[3] Golub VV., Baklanov DI., Golovastov SV., Ivanov MF., Laskin .IN, Saveliev AS., et al. Mechanisms of high-pressure hydrogen gas self-ignition in tubes. Journal of Loss Prevention in the Process Industries 2008; 21(2):185-198.

[4] Mogi T., Kim D., Shiina H., Horiguchi S., Self-ignition and explosion during discharge of high-pressure hydrogen. Journa lof Loss Prevention in the Process Industries2008;21 (2):199-204.

[5] J. Grune, M. Kuznetsov, K. Sempert, T. Jordan, Experimental study of ignited unsteady hydrogen releases from a high pressure reservoir. Proceedings to the 4th International Conference of Hydrogen Safety, San Francisco, USA, 2011, pp. 132–7A3.

[6] M. Brouillette, Shock waves at microscales, Shock Waves (2003) 13: 3–12.

[7] Russell E. Duff, ShockTube Performance at Low Initial Pressure, Phys. Fluids 2, 207 (1959).

[8] S. Golovastov, V. Bocharnikov, The influence of diaphragm rupture rate on spontaneous selfignition of pressurized hydrogen: Experimental investigation. International journal of hydrogen energy 37 (2012) 10956-10962

[9] Y.R. Kim, H.J. Lee, S. Kim, I.S. Jeung A flow visualization study on self-ignition of high pressure hydrogen gas released into a tube Proc Combust Inst (2012)

[10]Goodwin, D.G., Cantera User's Guide, California Institute of Technology, Pasadena, CA, November, 2001

[11]Lutz, A.E., Sandia Report SAND88-8228 (1988).

K.A. Bhaskaran, M.C. Gupta, T. Just, Combust. Flame 21 (1973) 45–48.